Free-Electron Lasers: Status and Applications

Patrick G. O'Shea[1] and Henry P. Freund[2]

A free-electron laser consists of an electron beam propagating through a periodic magnetic field. Today such lasers are used for research in materials science, chemical technology, biophysical science, medical applications, surface studies, and solid-state physics. Free-electron lasers with higher average power and shorter wavelengths are under development. Future applications range from industrial processing of materials to light sources for soft and hard x-rays.

Free-electron lasers (FELs) are capable of operation over the entire electromagnetic spectrum and are rapidly filling spectral voids left by conventional sources (*1*). They have been operated from the microwave to the vacuum ultraviolet regions, at average powers up to several kilowatts and peak powers up to a gigawatt. At present, there are two principal areas for future FEL development: higher average power and shorter wavelengths.

FELs consist of an electron beam propagating through a periodic magnetic field (called a wiggler or undulator) (Fig. 1). Undulators are also used in incoherent synchrotron light sources. Lasing occurs because the wiggler and the radiation combine to produce a beat wave (essentially an interference pattern called a ponderomotive wave) that travels slower than the speed of light and can be in synchronism with the electrons. A good analogy is a group of surfers and a wave. If the surfers remain stationary, the velocity difference between them and the wave is large, and an incoming wave merely lifts them up and down in passing. But if they "catch the wave" by paddling to match velocities, then they can gain energy from the wave. This is the physical basis of an FEL, except that the electron phase is chosen to amplify the wave, so the situation is more analogous to the surfers "pushing" on the wave and increasing its amplitude.

The discrete energy levels existing in conventional lasers are not a factor in FELs, where electron energy transitions occur in a continuum. The thermal energy that heats the lasing medium is carried away at acoustic velocities ($\sim 10^3$ m/s) in conventional lasers but at near-lightspeed ($\sim 10^8$ m/s) in an FEL. As such, FELs are more akin to traveling-wave tubes than to conventional lasers. In addition, the FEL is continuously tunable, is capable of high peak and average powers, and can produce a wide variety of pulse formats. These recent developments in FELs represent a resurgence of vacuum electronic devices as sources of coherent radiation (*2*).

The average power of FELs is increasing. In continuous mode, a record average power of 1.7 kW has been produced at a wavelength of 3 μm (*3*). Similar power levels of up to 2 kW over a 1-ms macropulse have also been produced in the infrared (*4*). The high average power goal is several tens of kilowatts at infrared to ultraviolet wavelengths. The most likely configuration is an oscillator driven by a radio-frequency linear accelerator (rf linac). Rates of development of vacuum generators of coherent radiation can be gauged by using the power density (the product of the average power and the square of the radiation frequency) as a figure of merit. The evolution of power densities in magnetrons, klystrons, gyrotrons, and FELs (Fig. 2) (*5*) shows that rapid magnetron development began in the 1940s and reached its limits by about 1950, after which klystron development followed a similar pattern through the mid-1970s. The beam tunnels are larger in gyrotrons and FELs and result in increased power-handling capacity. Although technological limits for each device exist, the envelope for different devices increases exponentially and yields a rough estimate for the rate of progress. The limits for FELs have not yet been reached, and a project is under construction at the Thomas Jefferson Laboratory (*3*) to reach 10 kW.

Tunable, hard x-ray FELs (*6, 7*) have been proposed as fourth-generation light sources. The major advantage of FELs is that they produce coherent light many orders of magnitude brighter than the incoherent light produced in synchrotrons, which were used for the previous three generations of light sources. Short-wavelength FELs are primarily directed toward x-ray research applications at wavelengths down to 1 Å, and this is illustrated by the peak brilliance of a wide range of the present-day synchrotrons and the projected performance of FELs (Fig. 3) (*7*). Consequently, applications in the x-ray region will undergo an upheaval similar to that which followed the invention of the laser at visible wavelengths.

Ultraviolet FEL oscillators using electron storage rings are currently in operation (*8*). The electron beam quality in modern rings is excellent, making them suitable as drivers for visible and ultraviolet FELs. But limitations on beam emittance, current, and mirror technology appear to limit the smallest achievable wavelength to ~100 Å in storage-ring FELs (*8*).

One scheme not requiring mirrors is referred to as self-amplified spontaneous emission (SASE). Here, shot noise on the electron beam is amplified in a single pass through a long wiggler. All the x-ray FELs shown in Fig. 3 are in this category. However, alternate schemes are also possible. For example, if progress in other types of x-ray lasers continues (*9*), then a master oscillator power amplifier (MOPA) is possible. In addition, harmonic generation schemes are under study at Brookhaven (*10*) and Argonne National Laboratories (*11*) in which a seed laser at a subharmonic of the desired output wavelength is used to start the amplification process.

History of Free-Electron Lasers

Spontaneous emission at visible wavelengths and coherent radiation of microwaves was demonstrated (*12*) in the early 1950s using an rf linac and a wiggler. Between 1957 and 1964, a free-electron maser was demonstrated, called a "ubitron" (for undulating beam interaction), that produced peak powers of 150 kW at a wavelength of 5 mm (*13*). FEL research then languished until the 1970s, when it resumed from two different but complementary approaches relying on stimulated Compton and Raman scattering, respectively. The Compton scattering regime occurs when the electron current is sufficiently small that the beam space-charge potential is smaller than the ponderomotive potential; the Raman scattering regime occurs when the electron current is sufficiently large that the beam space-charge potential is larger than the ponderomotive potential. In 1971, an optical device subsequently referred to as a "free-electron laser" was proposed (*14*) that would operate in the

[1]Department of Electrical and Computer Engineering and Institute for Plasma Research, University of Maryland, College Park, MD 20742, USA. [2]Science Applications International Corporation, McLean, VA 22102, USA.

Compton regime and sparked experiments in near-infrared amplifiers (*15*) and oscillators (*16*). Raman FELs were pioneered at numerous laboratories around the world (*17–19*) and operated at microwave and millimeter wavelengths. These were the first SASE FELs, although the term "superradiant amplifiers" was commonly used.

Early SASE development occurred at wavelengths from microwaves through the far infrared (roughly from 6 mm down to 600 μm), and these devices operated either in the Raman or borderline Raman/Compton regimes. As such, they typically used electron beams of relatively low energy (less than ~3.5 MeV) and high current (up to ~1 kA). These experiments demonstrated much of the essential physics, such as the constraints on electron beam brightness, the scaling of growth rates with beam and wiggler parameters, saturation of the SASE process, and shot-to-shot fluctuations in the output spectrum. Perhaps the most complete SASE experiment of this type was performed at a wavelength of 600 μm—that is, borderline between guided and optical propagation—and demonstrated good agreement between the observations and theory/simulation (*19*). In particular, the exponentiation of the power to saturation was observed directly and found to be in good agreement with simulation, and shot-to-shot fluctuations of 1 to 3% in the power and ±10% in the wavelength were observed. An output spectrum from this experiment is shown in Fig. 4.

The interest in x-ray SASE FELs (*20*) has fueled intense interest in infrared-, visible-, and ultraviolet-wavelength experiments to test the basic physics and technology. This activity was led by experiments that reported gain at wavelengths of 4 to 13 μm in the mid-infrared (*21*) and high gain at wavelengths of 15 to 16 μm (*22–24*). These experiments were made possible by the use of high-brightness photocathode electron guns and were stepping stones to shorter wavelengths. Experiments at visible (*25*) and vacuum ultraviolet (*26*) wavelengths have recently been reported.

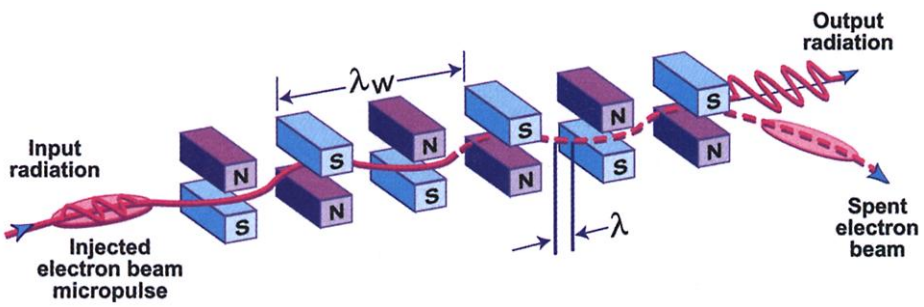

Fig. 1. Schematic illustration of the interaction between the electron beam and the wiggler in an FEL with a planar wiggler (*2*).

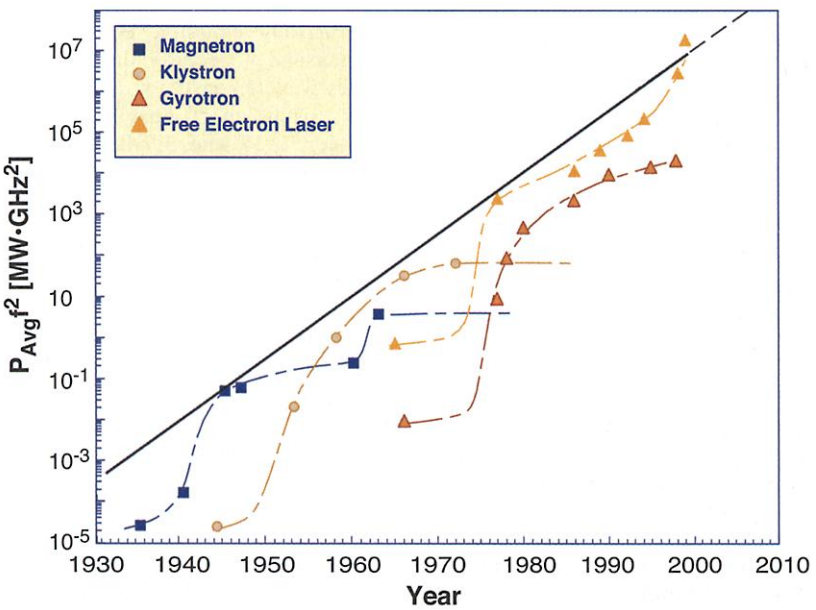

Fig. 2. Progress in the development of a variety of vacuum electronic sources of coherent radiation, as measured by the evolution of the product of the average power and the square of the frequency. [Adapted from (*2*)]

The experiments on the Low Energy Undulator Test Line (LEUTL) at Argonne National Laboratory were the first SASE FELs at visible and shorter wavelengths to reach saturation and to directly observe exponential growth (*27*). The latter was made possible by the use of a segmented wiggler permitting diagnostic stations to be placed in the gaps between the wigglers. The results at a central wavelength of 5300 Å (Fig. 5) were obtained from an ensemble of many individual shots and describe a bulk energy as well as a measure of the level of fluctuations about this value. The asymmetry reflects the skewed nature of the shot-to-shot statistics. The line is the result of a numerical simulation. The exponentiation is evident in the data, and the saturated power is estimated to reach ~30 MW. The simulation results were normalized to pass through the first data point, because uncertainties in the electron beam qualities make detailed energy comparisons difficult. More recently, saturation has been achieved in the ultraviolet at a wavelength of 3850 Å. In addition, first lasing was demonstrated at Deutsches Elektronen Synchrotron (*28*) at a photon energy of 11 eV and a peak brilliance of 6 (±4) × 10^{25} photons s^{-1} $mrad^{-2}$ mm^{-2} per 0.1% bandwidth.

Difficulties with SASE FELs could arise from fluctuations in the output spectrum. One alternative is a modular design using a seed laser at a low subharmonic of the desired frequency to start a chain of harmonic amplifications. This is possible because nonlinear harmonic growth in the FEL is driven strongly by bunching at the fundamental (*11, 29*) and can reach power levels of a few percent of the power at the fundamental. In this way the FEL is like many other vacuum electronic devices, whether high-voltage traveling-wave tubes or the gridded tubes used in vacuum-tube audio amplifiers.

One step toward this goal is a harmonic generation experiment (*10*) consisting of two wigglers separated by a magnetic chicane. A high-power seed laser tuned to be resonant with the first wiggler at 10.6 μm is injected in synchronism with the electron beam. This wiggler is not long enough to appreciably affect either the beam or the laser pulse, but it does begin bunching the electron beam that is subsequently enhanced in the dipole chicane. The electrons are then injected into the second wiggler that is tuned to the second harmonic of the seed laser, which, as a result of the prebunching, yields rapid growth of the harmonic. This experiment produced more than 20 MW at 5.3 μm. Building on this concept, and using the nonlinear harmonic mechanism to reach even higher harmonics, researchers have envisioned x-ray light sources built of a chain of such modules reaching successively shorter wavelengths at each step (*30, 31*).

The development of linac-based FELs with both higher power and shorter wave-

length was delayed by technological issues. In particular, the electron brightness was the principal limiting factor. The essential breakthrough was the development of laser-switched photocathode electron sources (photoinjectors) (*32, 33*) to replace thermionic cathodes, improving the electron beam brightness in rf linacs by two orders of magnitude. Photoinjectors are used routinely in short-wavelength FELs (*7, 27, 34*).

High average power FELs also benefited from the application of photoinjectors. In the early 1990s the average power record for an FEL was 11 W (*35*). An experiment at Boeing (*36*) demonstrated the ability of photoinjectors to produce high average electron beam power and high beam quality (160 kW, 5 MeV) with a photoinjector designed as a driver for a high-power FEL. Recovery of the energy from the spent electron beam is also an important technology for high average power applications and, when coupled with superconducting rf linacs, promises high average power FELs. These techniques were required to reach average power levels close to 2 kW in the mid-infrared (*3, 4*).

The Physics of Free-Electron Lasers

The wiggler mediates the interaction between the electrons and the photons in FELs. The intensity of incoherent radiation is proportional to the number of electrons per unit wavelength. Stimulated emission occurs when electrons form coherent bunches over a wavelength, and the number of emitted photons is then proportional to the square of the electron number. Bunching occurs because the ponderomotive wave has the same frequency (ω) as the radiation, but the wave number is the sum of the wave numbers of the electromagnetic (k) and wiggler (k_w) fields. Hence, the beat wave travels more slowly than the light wave and can be in synchronism with the electrons when the phase velocity of the ponderomotive wave equals the electron beam velocity (v_b), that is, $\omega/(k + k_w) = v_b$.

To understand how the ponderomotive wave is formed, consider the electron motion as illustrated in Fig. 6 (*1*) for a helical wiggler where the field is normal to the symmetry axis and rotates through 360° in one period. This exerts a force on the electrons acting at right angles to the direction of the field and the electron velocity that imposes a helical trajectory lagging 180° behind the wiggler phase. Both axial and transverse velocities have a constant magnitude, and the synchronous wavelength is

$$\lambda = (1 + a_w^2)\frac{\lambda_w}{2\gamma_0^2} = (1 + 0.872B_w^2\lambda_w^2)\frac{\lambda_w}{2\gamma_0^2} \quad (1)$$

where a_w ($\equiv eB_w/m_ec^2k_w^2$) is the wiggler strength parameter, the wiggler period λ_w is in centimeters, B_w denotes the wiggler amplitude (in teslas), and $\gamma_0 = 1 + E_b/m_ec^2$ for an electron kinetic energy E_b (where m_ec^2 is the electron rest energy). The direction of the ponderomotive force is given by the vector cross-product between the transverse electron velocity and the radiation magnetic field. When the phasing is correct, this direction opposes the axial streaming, yielding electron deceleration and wave amplification.

The interaction in a wiggler with planar symmetry is qualitatively similar; however, there are some differences because the transverse motion is planar and there is an oscillatory component to the transverse and axial velocities. Because of this, the root mean square wiggler magnitude determines the FEL performance. As such, the strength of a planar wiggler must be approximately $\sqrt{2}$ times that of a helical wiggler to have a comparable effect.

In general, amplification proceeds in

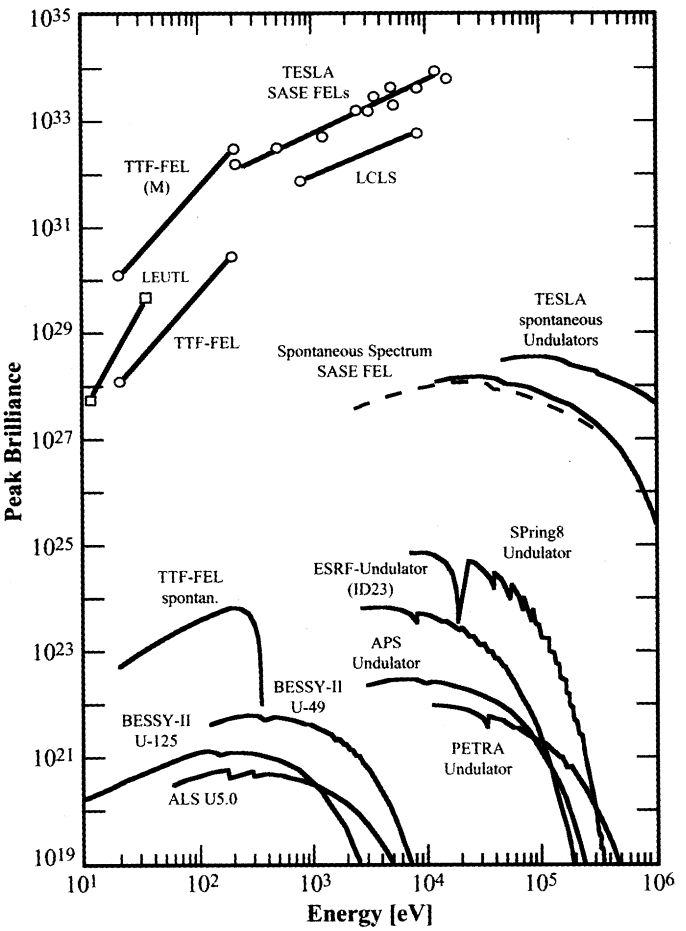

Fig. 3. Peak brilliance of x-ray FELs and undulators for spontaneous radiation at the TESLA Test Facility, in comparison with synchrotron radiation sources. Brilliance is expressed as photons s^{-1} $mrad^{-2}$ mm^{-2} per 0.1% bandwidth. For comparison, the spontaneous spectrum of x-ray FEL undulators is also shown. The label TTF-FEL indicates design values for the FEL at the TESLA Test Facility, with (M) for the planned seeded version (*28*).

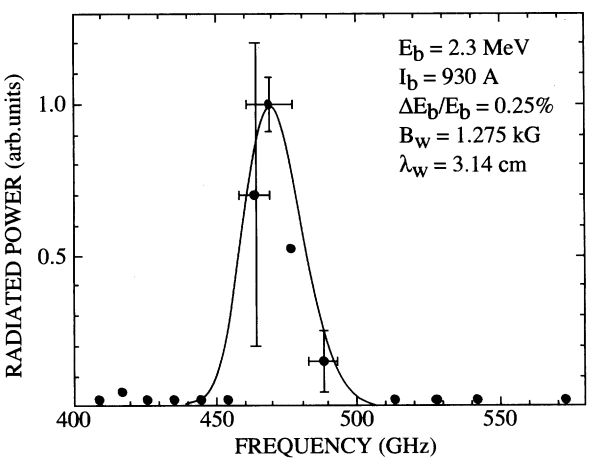

Fig. 4. The output spectrum from the 600-μm SASE FEL at MIT (*19*). The dots represent measurements; the curve is the result of simulation. The shot-to-shot fluctuations are reflected in the error bars.

three stages. Stage one is an initial low gain regime found near the start of the wiggler where the wave grows roughly as the cube of the distance. Stage two is exponential growth. The exponentiation (or gain) length is the distance over which the power increases by a factor of e (the base of the natural logarithms). The wiggler must be longer than several gain lengths to progress beyond the low gain regime. The third, nonlinear, stage begins once electrons become trapped in the ponderomotive wave. Saturation occurs when the number of trapped electrons losing energy to the wave is balanced by the electrons gaining energy from the wave. In low gain oscillators where the interaction does not progress beyond the low gain regime, the wave grows incrementally on each pass through the wiggler. However, the radiation grows to levels able to trap the electron beam after many passes through the wiggler, and the saturation mechanism is the same as when exponential growth occurs.

Diffractive losses in amplifiers and SASE FELs are important. For free space propagation, the radiation area doubles in one Rayleigh length and amplification ceases for light diffracting out of the beam. However, the electron beam guides the radiation by two related mechanisms known as gain and refractive guiding. Gain guiding is the preferential amplification in the region of the electron beam. Refractive guiding is radiation focusing due to the shift in the refractive index caused by the dielectric response of the electron beam. In other words, the FEL gain medium acts like an optical fiber to confine the light. However, optical guiding is not important in oscillators or at microwave wavelengths where the radiation is confined either by mirrors or by a waveguide.

Radiation growth can be adversely affected for pulsed electron beams by related effects called "slippage" and "lethargy." These effects occur because the group velocity is higher than the axial electron velocity and the beam lags behind the radiation pulse. Therefore, amplification of the leading edge of the pulse ceases, and the pulse subsequently begins to decay from wall losses and diffraction. Slippage is magnified because the electron beam slows the optical pulse below the group velocity in vacuo. In addition, the electron response is delayed because some distance is required to begin bunching before growth can begin in earnest. As a result, the leading edge of the optical pulse starts the bunching process, but the trailing edge benefits the most, causing a distortion of the optical pulse.

Slippage and lethargy are important considerations in oscillators using pulsed electron beams where the slippage time must be less than the pulse duration. For synchronization of the electron and optical pulses to occur, the separation time between beam pulses must equal the round-trip time of the optical pulses in the cavity. This is referred to as the cavity tuning. Because of the slowing of the optical pulse by the beam, the cavity length must be shorter than would be indicated by the round-trip time in the cavity in vacuo.

The efficiency depends on the specific configuration. For a low-gain oscillator, the efficiency (η) is inversely proportional to the number of wiggler periods (N_w), and $\eta \approx 1/2N_w$ and typical efficiencies range over about 1 to 2%. If the wiggler is tapered to compensate for electron deceleration, then much higher efficiencies can be obtained. The highest efficiency demonstrated at optical wavelengths is 5% at a wavelength of 10 μm (*37*). In principle, optical efficiencies up to 20% appear feasible. In high-gain MOPAs and SASE FELs, the efficiency is estimated by the requirement that the electrons lose an energy corresponding to twice the difference in the beam and ponderomotive phase velocities. Here, the efficiency is proportional to the product of the wiggler strength parameter to the 2/3 power and the cube root of the beam current, and is inversely proportional to the beam energy. For the x-ray SASE systems under consideration, the efficiencies are small, but peak powers of ~10 GW are nonetheless possible. Finally, the wallplug efficiency can be enhanced by energy recovery.

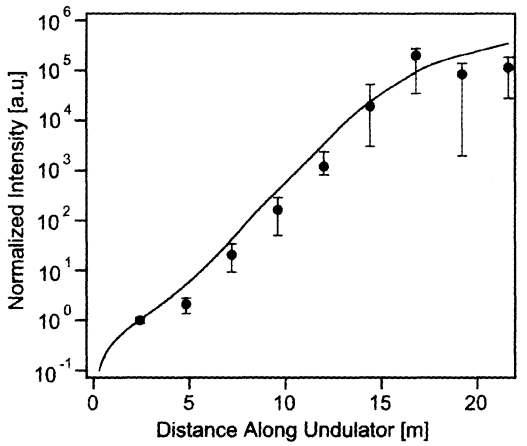

Fig. 5. The growth of the radiation (in arbitrary units) for the 5300 Å SASE FEL at Argonne National Laboratory (*27*). The data reflect shot-to-shot fluctuations as well as macroscopic variations in beam transport and detectors.

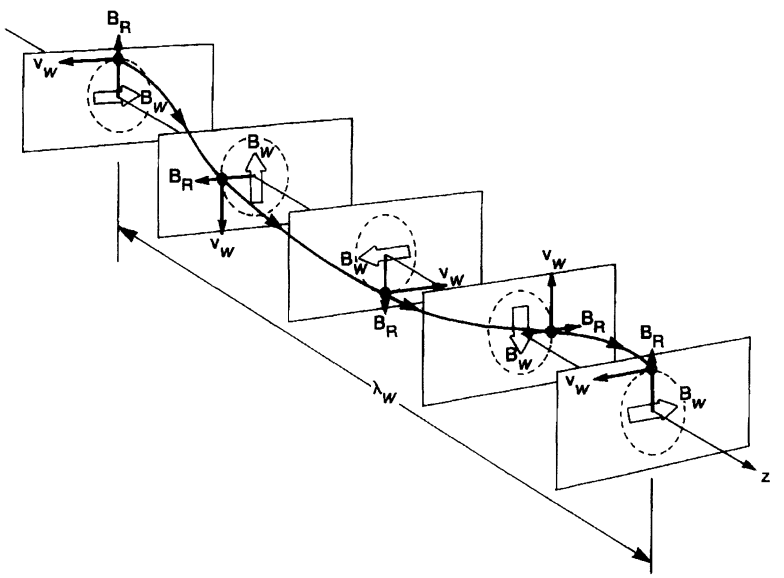

Fig. 6. Schematic illustration of the resonance condition between the beam and a wave in an FEL with a helical wiggler (*1*).

Basic and Applied Research with Free-Electron Lasers

As the FEL has matured, there has been substantial growth in the number of efforts to make use of the radiation. We cannot cover all areas of research under way or contemplated using FELs, but we can discuss broad categories. Several studies have examined the applicability of FELs to perform basic scientific research (*38, 39*). These have identified applications for which the FEL has no effective competition by virtue of the tunability, short pulse length, micropulse energy/

peak power, average power, ability to synchronize for pump probe efforts, bandwidth, and beam quality.

FELs excel as research tools at submillimeter and far-infrared wavelengths because they produce high-intensity pulses and have very little competition. Typical studies include measurements of principal excitations in condensed-matter systems, where it is possible to access the principal excitations such as plasmons, phonons, magnons, and intersubband transitions. Direct linear probing of defect modes and buried interfaces with bond specificity is possible (*40*). Measurement of energy distributions and line shapes can enable the investigation of mode coupling and energy dissipation into the electron or phonon continuum of the substrate. Low-frequency modes in large biomolecules such as nucleic acids and proteins can be excited in the far infrared for similar studies of energy flow.

Most existing FELs operate in the mid-infrared range. For many uses at wavelengths less than ~10 μm, existing tabletop lasers can satisfy most researchers' needs. Users turn to FELs when they need tunability, high repetition rates combined with high peak power, and a need for chirped (frequency-modulated) pulses. Optical parametric oscillators (OPOs) also tend to have bandwidths that are wide compared to their Fourier width. Despite the competition, this has been a fruitful range for researchers desiring to use the FEL. Many researchers synchronize the FEL output with another radiation source for measurements in this wavelength range. Examples of mid-infrared experiments taking advantage of the unique properties of FELs are studies of protein dynamics and hydrogen defect dynamics (*41*).

A particularly powerful technique is sum-frequency generation (SFG). Early examples include SFG measurements on the surface of Pt in methanol using 5-μm FEL pulses and a synchronized laser. In other tests, the FEL was used for pump probe observation of coherent transient grating effects of narrow-gap semiconductors and third-order nonlinearity coefficients and electron relaxation times in GaAs-AlGaAs quantum wells. SFG is also used to identify bonding and to monitor density when polyurethane is deposited on float glass, to show how the surface interaction modifies the fullerene geometry when fullerene is deposited on gold, and to characterize the vibrational dynamics of carbon monoxide at an electrochemical interface (*42*).

Studies in kinetics include vibrational energy transfers in molecules. This opens up a new class of experiments to study mode-selective chemistry that requires high-power short pulses that excite molecular vibrations. [For example, see (*43*) for isotope-selective multiphoton dissociation of formic acid and nitromethane.]

Second-order nonlinear susceptibility of the conduction band and valence band quantum well (QW) structures extracted from the interference between second harmonic fields of QWs and GaAs substrates has been studied by the azimuthal dependence of the second harmonic power. This was the first demonstration of difference frequency generation of mid-infrared in any QW (*44*).

Among the extensive studies carried out at the FELI facility in Japan (*45*) are resonant excitations of molecular vibrations, band discontinuities of semiconductor heterojunctions, and isotope separation. The user facilities at this lab have become among the most productive in the world, providing more than 2000 hours of beam time in the last year.

Surgical applications of FELs are being pursued. Studies at Vanderbilt University have shown that FEL wavelengths near 6.45 μm, corresponding to the amide II absorption band of proteins, are particularly well suited for soft tissue incision (*46*). In some cases, collateral damage extended only to a depth of 10 μm into the tissue from the cut boundary. The FEL has shown promise in its ability to successfully incise the optic nerve sheath in rabbits without cutting the underlying optic nerve (*47*). The first human FEL surgery was a biopsy of a benign brain tumor. Human trials of ocular surgery comparing an FEL to standard techniques of optic nerve sheath fenestration are now under way at Vanderbilt University. Researchers at FELI have also ablated and hardened dental materials and studied photodynamic therapy. The tunability, power, and pulse variability of the FEL has made it an efficient biophysical research tool.

Although there are numerous conventional lasers in the visible and near-ultraviolet ranges, FELs have an advantage when high average power is required and when cost per photon is an issue. Commercial applications have been proposed that use a high average power FEL to heat the surface of polymers for enhancements to the surface morphology. The key is to achieve very high average power (100 kW) at reasonable costs per photon (<$0.01/kJ). By enhancing surface roughness in polyester and nylon fibers, the resulting fabrics can be made softer, hydrophilic, and more readily accepting of dyes (*48*).

At the SuperACO storage ring FEL in France, operating at an average power of 0.1 W in the 3500- to 4300-Å range, time-resolved polarized fluorescence decays of the reduced nicotinamide adenine dinucleotide coenzyme NADH in aqueous solution using single photon counting were performed. The advantage of using an FEL on a storage ring is the natural synchronization with synchrotron emission in bending magnets. This was used to study relaxational dynamics of the excited state. In other experiments, the surface photovoltage effect on Si(111) and the resulting modification of electronic band bending using time-resolved photoemission (*49*) were measured. Current efforts include photo-ionization of excited helium, FEL excitation of photocarriers and production of photofragments in the infrared, and transient absorption in excited tumor cells.

In the x-ray region, a series of experiments using the Linac Coherent Light Source (LCLS) have been proposed (*39*) at wavelengths from 1.5 to 15 Å in which the FEL is used as a nondestructive probe, to induce nonlinear interactions, or to produce matter under extreme conditions of temperature and pressure. There are five general categories of proposed experiments: atomic physics, plasma and warm dense matter studies (matter with liquid or solid densities but temperatures comparable to the Fermi energy or with strongly coupled plasmas), structural studies on single particles and biomolecules, femtochemistry, and nanoscale dynamics in condensed matter.

In atomic physics, experiments such as multiple core hole formation in atoms (as indicated by the production of hypersatellite Auger electrons), multiphoton ionization of K-shell electrons, and giant Coulomb explosions in atomic clusters are possible.

At present, radiation damage is a limiting factor in structural studies of biological samples. Most such studies using x-rays rely on crystalline forms of biomolecules to amplify a signal by Bragg reflections, and hence are limited to macromolecules that can be crystallized. At the high fluxes anticipated, nanocrystals, nanoclusters of proteins, and viruses can be studied. X-ray diffraction tomography of whole cells is possible. With very short high-intensity x-ray pulses, it may be possible to perform biomolecular imaging on single large molecules before damage-induced movements destroy the samples (*50*). The elimination of the requirement for crystals would remove a major research bottleneck.

The proposed x-ray FELs will have resolution on the scale length of molecular bonds and the time scales of molecular vibrations. This would permit direct observation of reaction processes such as the photodissociation of isolated gas-phase molecules, photochemically induced bond breakage and recombination, and structural transformations in photosynthetic processes. Studies of nanoscale dynamics involve the overlap of different time and length scales. Techniques that will be possible include x-ray photon correlation spectros-

copy and x-ray transient grating spectroscopy, which can be used to study the dynamics of entangled polymers, glassy dynamics, and collective mode dynamics in liquids and gases.

Summary

Major new FEL projects are on the drawing boards that point the way to exciting new applications of this technology. The demonstration of 2 kW average power in the near infrared (*3*) has opened the door for high average power applications in materials processing. Continued development of high-power FEL technology in the ultraviolet should produce considerable interest from industry. Ultrashort-wavelength FELs will be an important component in the next generation of light sources that will produce coherent, short-pulse radiation of soft and hard x-rays. The technical challenges are particularly great in this region, but recent developments in linear accelerator and storage ring technology have made the new frontiers both alluring and reachable.

FELs will also be important in the far infrared at wavelengths of several tens to several hundred micrometers, where there is a paucity of intense, short-pulse sources. Many molecular resonances of biological interest that have not yet been investigated are in this region. These FELs can be very compact, will fit on an optical bench, and will be suitable for individual investigator use.

References and Notes

1. H. P. Freund, T. M. Antonsen Jr., *Principles of Free-Electron Lasers* (Chapman & Hall, London, ed. 2, 1996).
2. H. P. Freund, G. R. Neil, *Proc. IEEE* **87**, 782 (1999).
3. G. R. Neil *et al.*, *Phys. Rev. Lett.* **84**, 662 (2000).
4. E. J. Minehara *et al.*, *Nucl. Instrum. Methods* **A445**, 183 (2000).
5. This is updated from a plot that appeared in R. K. Parker, R. H. Abrams Jr., *Proc. SPIE* **791**, 2 (1987).
6. LCLS Design Group, *LCLS Design Report* (NTIS Doc. No. DE98059292, National Technical Information Service, Springfield, VA, 1998).
7. J. Rossbach, *Nucl. Instrum. Methods* **A375**, 269 (1996).
8. M. Poole, *Synchrotron Radiat. News* **13**, 4 (2000).
9. D. Korobkin *et al.*, *Phys. Rev. Lett.* **81**, 1607 (1998).
10. L. H. Yu *et al.*, *Science* **289**, 932 (2000).
11. H. P. Freund *et al.*, *IEEE J. Quantum Electron.* **36**, 275 (2000).
12. H. Motz *et al.*, *J. Appl. Phys.* **24**, 826 (1953).
13. R. M. Phillips, *Nucl. Instrum. Methods* **A272**, 1 (1988).
14. J. M. J. Madey, *J. Appl. Phys.* **42**, 1906 (1971).
15. L. R. Elias *et al.*, *Phys. Rev. Lett.* **36**, 717 (1976).
16. D. A. G. Deacon *et al.*, *Phys. Rev. Lett.* **38**, 892 (1977).
17. V. L. Granatstein *et al.*, *Appl. Phys. Lett.* **30**, 384 (1977).
18. T. J. Orzechowski *et al.*, *Phys. Rev. Lett.* **54**, 889 (1985).
19. D. A. Kirkpatrick *et al.*, *Phys. Fluids B* **1**, 1511 (1989).
20. R. Bonifacio, C. Pellegrini, L. M. Narducci, *Opt. Commun.* **50**, 359 (1984).
21. R. Prazeres *et al.*, *Phys. Rev. Lett.* **78**, 2124 (1987).
22. M. Hogan *et al.*, *Phys. Rev. Lett.* **80**, 289 (1998).
23. D. C. Nguyen *et al.*, *Phys. Rev. Lett.* **81**, 810 (1998).
24. A. Tremaine *et al.*, *Phys. Rev. Lett.* **81**, 5816 (1998).
25. S. V. Milton *et al.*, *Phys. Rev. Lett.* **85**, 988 (2000).
26. J. Andruszkow *et al.*, *Phys. Rev. Lett.* **85**, 3825 (2000).
27. S. V. Milton *et al.*, *Science*, in press.
28. J. Rossbach, personal communication.
29. Z. Huang, K. J. Kim, *Phys. Rev. E* **62**, 7295 (2000).
30. S. G. Biedron *et al.*, *Nucl. Instrum. Methods*, in press.
31. J. Wu, L. H. Yu, *Nucl. Instrum. Methods*, in press.
32. R. L. Sheffield, in *AIP Conference Proceedings 184* (1988), vol. 2, pp. 1500–1531.
33. K. Batchelor *et al.*, *Nucl. Instrum. Methods* **A318**, 372 (1992).
34. P. G. O'Shea *et al.*, *Phys. Rev. Lett.* **71**, 3661 (1993).
35. C. A. Brau, *Nucl. Instrum. Methods* **A318**, 38 (1992).
36. D. H. Dowell *et al.*, *Appl. Phys. Lett.* **63**, 2035 (1993).
37. D. W. Feldman *et al.*, *Nucl. Instrum. Methods* **A285**, 11 (1989).
38. National Research Council, "Free electron lasers and other advanced sources of light," in *Report of the Committee on Free Electron Lasers* (National Academy Press, Washington, DC, 1994).
39. For more information on the proposed LCLS experiments, see www-ssrl.slac.stanford.edu/lcls.
40. S. J. Allen *et al.*, *Nucl. Instrum. Methods* **A358**, 536 (1995).
41. M. Budde *et al.*, *Phys. Rev. Lett.* **85**, 1452 (2000).
42. A. Peremans *et al.*, *Nucl. Instrum. Methods* **A375**, 657 (1996).
43. A. K. Petrov *et al.*, in *FEL and Its Applications in Asia*, T. Tomimasu, E. Nishimika, T. Mitsuyu, Eds. (Ionics, Tokyo, 1997), p. 245.
44. H. C. Chui *et al.*, *Appl. Phys. Lett.* **66**, 265 (1995).
45. T. Tomimasu *et al.*, in *FEL and Its Applications in Asia*, T. Tomimasu, E. Nishimika, T. Mitsuyu Eds. (Ionics, Tokyo, 1997), p. 65.
46. G. Edwards *et al.*, *Nature* **371**, 416 (1994).
47. K. Joos *et al.*, *Lasers Surg. Med.* **27**, 191 (2000).
48. M. J. Kelley, *Proceedings of SPIE Conference (FEL Challenges)*, 13 to 14 February 1997, San Diego, CA (SPIE Press, Bellingham, WA, 1997), pp. 240–244.
49. M. E. Couprie *et al.*, *Nucl. Instrum. Methods* **A375**, 639 (1996).
50. R. Neutze, *Nature* **406**, 752 (2000).

51. Funded in part by a grant from the U.S. Naval Research Laboratory.